Glucose-sensing in AgRP neurons integrates homeostatic energy state with dopamine signalling in the striatum.

Alex Reichenbach[1], Rachel E Clarke[1], Romana Stark[1], Sarah Haas Lockie[1], Mathieu Mequinion[1], Felicia Reed[1], Sasha Rawlinson[1], Harry Dempsey[1], Tara Sepehrizadeh[2], Michael DeVeer[2], Astrid C Munder[1,3], Juan Nunez-Iglesias[5], David C. Spanswick[1,9], Randall Mynatt[6], Alexxai V. Kravitz[8], Christopher V. Dayas[7], Robyn Brown[3,4], Zane B. Andrews[1].

1. Monash Biomedicine Discovery Institute and Department of Physiology, Monash University, Clayton 3800, Victoria, Australia
2. Monash Biomedical Imaging Facility, Monash University, Clayton 3800, Victoria, Australia
3. Florey Institute of Neuroscience & Mental Health, Parkville 3052, Victoria, Australia
4. Department of Biochemistry and Pharmacology, University of Melbourne, Parkville 3010, Victoria, Australia.
5. Monash Biomedicine Discovery Institute and Department of Anatomy and Developmental Biology, Monash University, Clayton 3800, Victoria, Australia
6 Gene Nutrient Interactions Laboratory, Pennington Biomedical Research Center, Louisiana State University System, Baton Rouge, Louisiana, USA
7 School of Biomedical Sciences and Pharmacy, University of Newcastle, 2308, NSW, Australia
8 Departments of Psychiatry, Anesthesiology, and Neuroscience, Washington University in St Louis, St Louis, MO, US
9 Warwick Medical School, University of Warwick, Coventry CV4 7AL, UK

Corresponding author:
Prof Z. B. Andrews: Email: Zane.Andrews@monash.edu Tel: +61 3 9905 8165

Disclosure Statement: The Authors have nothing to disclose

Acknowledgements:
This study was supported by an NHMRC grant and fellowship to ZBA (1126724, 1154974). We would like to thank Miles Billard from TDT for his valuable technical assistance and support with setting up photometry and analysis. The authors acknowledge the facilities and scientific and technical assistance of the National Imaging Facility, a National Collaborative Research Infrastructure Strategy (NCRIS) capability, at Monash Biomedical Imaging, Monash University. We would like to thank Professor Alex Fornito for the use of fDOPA in PET studies. We acknowledge that Bio Render was used to produce elements incorporated in the figure and graphical abstract (Biorender.com).

ABSTRACT

Hunger increases the motivation of an organism to seek out and consume highly palatable energy dense foods by acting on the midbrain dopaminergic system. Here, we identify a novel molecular mechanism through which hunger-sensing AgRP neurons detect low energy availability and modulate dopamine release to increase motivation for food reward.

We tested the hypothesis that carnitine acetyltransferase (Crat), a metabolic enzyme regulating glucose and fatty acid oxidation, in AgRP neurons is necessary to sense low energy states and regulate motivation for food rewards by modulating accumbal or striatal dopamine release. In support of this, electrophysiological studies show that AgRP neurons require Crat for appropriate glucose-sensing. Intact glucose-sensing in AgRP neurons controls post-ingestive dopamine accumulation in the dorsal striatum. Fibre photometry experiments, using the dopamine sensor $GRAB_{DA,}$ revealed that impaired glucose-sensing, in mice lacking Crat in AgRP neurons, reduces dopamine release in the nucleus accumbens to palatable food consumption and during operant responding, particularly in the fasted state. Finally, the reduced dopamine release in the nucleus accumbens of mice lacking Crat in AgRP neurons affects sucrose preference and motivated operant responding for sucrose rewards. Notably, these effects are potentiated in the hungry state and therefore highlight that glucose-sensing by Crat in AgRP neurons is required for the appropriate integration and transmission of homeostatic hunger-sensing to dopamine signalling in the striatum. These studies offer a novel molecular target to control the overconsumption of palatable foods in a population of hunger-sensing AgRP neurons.

INTRODUCTION

The motivation to approach and consume food depends not only on the palatability and caloric density of the available food source, but also on the energy state of the organism. For example, when food is abundant many prey species forage within known terrorities to reduce survival threats[1]. Conversely, when food is scarce, animals are motivated to take greater risks and forage within unfamiliar territories to search for food[2]. Thus, the motivation to seek palatable, energy-dense food evolved as a key mechanism for survival and maturation in an environment with limited food availability. Given that heightened motivation for palatable food in an environment of low food availability shaped an evolutionary benefit, it is not surprising that homeostatic feeding circuits responding to energy state can have a profound effect on motivation. In today's society with high caloric foods readily available, these circuits may contribute to the overconsumption of highly palatable and calorie dense foods, which is a leading cause for today's obesity crisis. Indeed, human evidence shows that fasting biases reward systems to high caloric foods[3,4].

Agouti-related peptide (AgRP) neurons in the arcuate nucleus of the hypothalamus (ARC) are a critical population of hunger-sensitive neurons that primarily function to increase appetite or conserve energy[5-9]. A key element of appetitive behaviour is the increased motivation for goal-directed outcomes. Intriguingly, hunger associated with fasting or calorie restriction has been used for decades in behavioural neuroscience to improve performance and learning in operant tasks. AgRP neurons function within this framework by increasing the willingness to work for food and food rewards. For example, activation of AgRP neurons makes mice more willing to work for food or food rewards at the same level as that seen in fasted mice[7,10-12]. Moreover, AgRP neurons transmit energy-state information to circuits involved in motivation[13-15], with the activation of AgRP neurons elevating dopamine release in response to food availability[13]. Given that AgRP neurons are most active during periods of energy deficit[16-20], they are a critical neural population that transmits low energy, hunger-specific metabolic information to motivation circuits. However, a fundamental gap in knowledge exists; what are the molecular mechanisms that enable AgRP neurons to sense changes in energy-state and integrate this metabolic information into neural circuits that reinforce food value and motivate feeding behaviours?

Sensory cues that predict food availability and palatability rapidly suppress hunger-sensitive AgRP neuronal activity in hungry mice[11,18,21,22]. Although this decrease in activity occurs prior to food consumption, post-ingestive caloric feedback is required to sustainably reduce AgRP neuronal activity[22,23], as this effect was not observed after repeated ingestion of a non-caloric sweetened gel. Su et al show also that the reduction of AgRP neuronal activity correlates with the number of calories ingested[22]. These studies highlight that the maintenance of normal AgRP activity in response to post-ingestive gastrointestinal feedback

requires metabolic sensing of available calories in combination with gut-brain neural communication[22-24]. Given that AgRP neurons increase food motivation by engaging midbrain dopamine circuits and require appropriate metabolic sensing of available calories for their normal function, we hypothesized that metabolic sensing of calorie availability is necessary for AgRP neurons to transmit energy-state information to pathways that control motivated behaviour towards a palatable food reward.

Previously we demonstrated that carnitine acetyltransferase (Crat) in AgRP neurons was required as a molecular sensor for peripheral substrate utilisation during fasting and refeeding[25]. Moreover, Crat in AgRP neurons programmed a broad metabolic response of the AgRP proteome and was required to promote normal refeeding after fasting[25]. Given this reduced appetitive drive in KO mice, we hypothesised that Crat in AgRP neurons would translate metabolic information about low energy state into neural circuits controlling dopamine signalling and the motivational aspects of food-directed behaviour.

Here we describe experiments demonstrating that Crat is important for glucose-sensing in AgRP neurons. Moreover, the absence of Crat in AgRP neurons reduced motivated behaviour during an operant task and dopamine release in the nucleus accumbens (NAc) during operant responding for and consumption of a palatable food reward. These studies highlight that glucose-sensing by Crat in AgRP neurons is required for the appropriate integration of hunger-sensing to potentiate food reward-related dopamine release in the NAc and control motivation for palatable food rewards.

Methods

Animals

All experiments were conducted in compliance with the Monash University Animal Ethics Committee guidelines. Male and female mice were kept under standard laboratory conditions with free access to food (chow diet, catalog no. 8720610, Barastoc Stockfeeds, Victoria, Australia) and water at 23C in a 12-hr light/ dark cycle and were group-housed to prevent isolation stress unless otherwise stated. All mice were aged 8 weeks or older for experiments unless otherwise stated. AgRP-ires-cre mice were obtained from Jackson Laboratory AgRP$^{tm1(cre)Low/J}$ (stock no. 012899) and bred with NPY GFP mice (B6.FVB-Tg(Npy-hr*GFP*)1Lowl/J; stock number 006417; The Jackson Laboratory, Maine, USA). AgRP-ires-cre::NPY GFP mice were then crossed with Crat$^{fl/fl}$ mice donated by Randall Mynatt (Pennington Biomedical Research Center, LA, USA) in order to delete Crat from AgRP neurons (AgRP$^{cre/wt}$::Crat$^{fl/fl}$ mice; designated as KO). AgRP$^{wt/wt}$::Crat$^{fl/fl}$ littermate mice were used as control animals (designated as WT)

Electrophysiology

Animals were fasted overnight and 250 µm thick coronal hypothalamic brain slices containing the ARC were prepared from 10 male AgRP Crat KO and 9 WT mice (8-12 weeks) expressing GFP in NPY neurons, and stored at room temperature before transferral to the recording chamber. Slices were continuously superfused at 4-5 ml/min with oxygenated (95% O_2, 5% CO_2) artificial cerebrospinal fluid (aCSF) of the following composition (in mM): NaCl 127, KCl 1.9, KH_2PO_4 1.2, $CaCl_2$ 2.4, $MgCl_2$ 1.3, $NaHCO_3$ 26, D-Glucose 2, Mannitol 8 (310 mOsm, pH 7.4). Hypothalamic neurons were visualised under IR illumination using a 63x or 40x water immersion objective on an upright microscope (Axioskop 2, Zeiss) and an Axiocam MRm camera (Zeiss). AgRP neurons were identified using a GFP filter set. Patch pipettes (8-11 MΩ) were pulled from borosilicate glass capillaries (Harvard Apparatus) and filled with intracellular solution containing (in mM): K-gluconate 140, KCl 10, EGTA 1, HEPES 10, Na-ATP 2, Na-GTP 0.3 (300 mOsm and pH 7.3, adjusted with KOH). Whole-cell current clamp recordings were made using the MultiClamp 700B amplifier, digitized with the Digidata 1550B interface, and acquired in pClamp 10.6 at 5 kHz sampling rate (Axon Instruments). To test the influence of an elevated extracellular glucose concentration on neural activity, aCSF was prepared as described above with the following changes: D-Glucose 5mM, Mannitol 5mM, and bath-applied for 10-15min. Data were analysed in Clampfit 10.6 (Axon Instruments) and plotted in Graphpad Prism 8.3. Figures were further prepared in Adobe Illustrator CC 2020.

Two bottle choice tests

Male and female mice were single housed in BioDaq feeding cages with *ad libitum* access to chow and two water bottles. After 3 days of acclimatisation, one bottle was filled with 0.1% saccharin and position of bottles swapped daily. After 4 days *ad libitum* feeding, mice were overnight fasted with only access to drink bottles followed by 2 days wash out period with ad lib access to water and chow. In the same manner mice were presented with choice of 4% sucrose and 0.1% saccharin solutions in week 2 and 4% sucrose laced with quinine HCl (concentrations for different cohorts ranging from 0.1 to 0.5mM) and 0.1% saccharin in week 3 of the experiment.

PET/CT and MRI

Mice were single housed and trained to receive a single Reese's® peanut butter chip 6 hours into the light phase (time of PET scan) for 1 week. The day before PET/CT scans, mice were fasted overnight (18 hours) with ad lib access to water. On the experimental day, mice were injected IP with 10mg/kg Benserazide (Selleckchem.com) and 10mg/kg Entacapone (Selleckchem.com) 30 minutes before injecting radiolabelled fDOPA (approx. 5MBq) into the tail vein. After 5 min rest, mice received 1 peanut butter chip and only those mice that initiated feeding with the first minute were included in the analysis. Then mice were anaesthetised (1-2.5% isoflurane) and a 65 min PET/CT scan was performed under anaesthesia. The scan was acquired using the Inveon scanner (Siemens Inveon). CT was generated using the following parameters: 97µm of resolution, 80kV voltage and 500uA current, mainly for attenuation correction and MRI overlaying purposes. PET scans were acquired for 60 minutes (16 time frames). One week later MRI scan was performed on these animals to generate T2 weighted images using these parameters: 3D Flash sequence, TE/TR=8/60ms, 4 averages, flip angle= 10 degree, resolution = 0.155 mm^3, scan time 20 minutes. PET images were analysed using IRW software (Inveon Research Workplace 4.2). PET/CT images were overlaid manually with the T2-Weighted images. Region of Interests (ROIs) were generated carefully by one investigator (AR) on the T2 images on left/right ventral striatum, left/right dorsal striatum and cerebellum (according to Allen brain atlas) and PET voxel intensities (Unit Bq/ml) at 3 different time points were exported for further analysis. We specifically choose to use the ventral striatum, rather than the NAc, due to greater accuracy with ROI identification. SUV (Standardized Uptake Value) of ROIs were calculated for each time point using the following equation:

$SUV = C_{PET}(T)/(Dose/Weight)$

$C_{PET}(T)$ = Tissue radioactivity concentration at time T

Dose= administration dose at time of injection (decay corrected to the time points)

Weight= animal body weight

To eliminate bias for slight variation of size/location of ROI we used upper bound Bq/ml values to calculate SUVmax[26] and normalised to cerebellum as reference:

SUVRmax= SUVmax target/SUVmax reference

Fiber photometry

Mice for fiber photometry experiments were anesthetised (2-3% isoflurane) and injected with Metacam (5 mg/kg) prior to placing into stereotaxic frame (Stoelting/Kopf) on heatpad (37C) and viral injections were performed as previously described[27]. Non-cre dependent dopamine sensor (YL10012-AAV9: AAV-hSyn-DA4.3)[28] was injected (2x150nl @25nl/min, 5 min rest) in dorsal striatum (bregma 0.5mm, midline 1.3 mm. skull -3.4mm) or NAc (bregma 1.2mm, midline 0.5 mm. skull -4.8mm) and ferrule capped fibres (400µm core, NA 0.48 Doric, MF1.25 400/430-0.48) implanted above injection site and secured with dental cement (GBond, Japan). Mice had 2 weeks recovery before commencement of experiments.

All fiber photometric recordings were performed with a rig using optical components from Doric lenses controlled by Tucker Davis Technologies fiber photometry processor RZ5P. TDT Synapse software was used for data acquisition. Prior to experiments, baseline dopamine signal was measured and LED power was adjusted for each mouse to achieve approximately 200mV for 465nm and 100mV for 405nm. Data analysis was done using modified python code provided by TDT[29,30]. The modified code is available at github/AlexReichenbach upon publication. Briefly, raw traces were down sampled and fitted to detrend signal bleaching and z-scores around precisely timed TTL-triggered events were extracted. To measure dopamine release to non-food-object/chow/peanut butter chip, single-housed mice with fiber implants were habituated to receiving Reese's® peanut butter chips in the home cage. On the test day mice were connected to fiber photometry setup in their home cage and a small ceramic bowl placed inside. Recording started after 5 minutes acclimation period. In 2 minute intervals a small wood dowel (novel non-food object), a chow pellet, and a peanut butter chip were dropped into the ceramic bowel in that order. Mice were fed or fasted in random cross over design.

Operant conditioning task

For operant conditioning experiments, Feeding Experiment Devices version 3 (FED3)[31] were placed overnight (16h) inside home cages under *ad libitum* conditions trained to reliably nose poke on fixed ratio (FR)1, FR3 and FR5 schedules (criteria to move to higher schedule was 3 consecutive days over 75% correct nose pokes) The dispensing of a sugar pellet (20mg, 65% sucrose, 5TUT Test Diets, Saint Louis, Missouri, USA) was paired with an LED light cue. During these FR sessions, a nose poke in the 'active' hole resulted in the delivery of a sugar pellet and was paired with a LED light cue whereas a nose poke in the 'inactive'

hold resulted in no programmed response. Importantly, mice were never food restricted during training to prevent this confounding the interpretation of our results. Once stable operant responding was established (> 75% correct nose pokes on FR5) mice were placed on a progressive ratio (PR) schedule under *ad libitum* fed conditions for a single overnight PR session (16 h). PR sessions were based on a Richardson Roberts schedule[32] where the number of pokes required to obtain a reward increased after every completed trial in the following pattern; 1, 2, 4, 6, 9, 12, 15, 20, 25, 32, etc. After this single PR session, stable FR5 responding was re-established (>75% correct nose pokes, typically 1 FR session) and a second PR session was performed except this time mice were fasted 16h prior to the PR session. Separate cohorts with fiber implants in the dorsal striatum or NAc were trained to receive sugar rewards as described above and dopamine responses to both nose pokes and sugar pellet retrieval were recorded in fed state or after an overnight fast.

Immunohistochemistry

To confirm viral injection and fiber placements, animals were deeply anesthetized with isoflurane and perfused with 0.05 M PBS, followed by 4% paraformaldehyde. Brains were postfixed in 4% paraformaldehyde overnight at 4°C then placed in 30% sucrose. Brains were cut at 40 µm on a cryostat, and every fourth section was collected and stored in cryoprotectant at −20°C. Sections were washed in 0.1 M phosphate buffer (PB), incubated with 1% hydrogen peroxide (H_2O_2) for 15 minutes to prevent endogenous peroxidase, activity, and blocked for 1 hour with 5% normal horse serum (NHS) in 0.3% Triton in 0.1 M PB. Sections were incubated with chicken anti-GFP (ab13970, Abcam) at 1:1000 in diluent of 5% NHS in 0.3% Triton in 0.1 M PB. After incubation, the sections were washed and incubated with Alexa Fluor goat anti-chicken 488 antibody (Invitrogen) at 1:500 in 0.3% Triton in 0.1 M PB. Sections were then washed, mounted, and coverslipped.

Statistical analysis

Statistical analyses were performed using GraphPad Prism for MacOS X. Data are represented as mean ± SEM. Two-way ANOVAs with post hoc tests were used to determine statistical significance. A two-tailed Student's unpaired t test was used when comparing genotype only. $p < 0.05$ was considered statistically significant.

RESULTS

Crat deletion impairs AgRP neuron glucose sensing

In order to demonstrate that Crat in AgRP neurons is important for glucose-sensing, we prepared hypothalamic brain slices from WT and KO mice for electrophysiological characterisation of glucose sensing in AgRP neurons. We detected no differences in the fundamental electrophysiological properties of AgRP neurons including resting membrane potential (Fig 1A), input resistance (Fig 1B), spontaneous firing frequency (Fig 1C), although peak action potential amplitude, was significantly lower in KO mice (Fig 1D). Collectively, these studies demonstrate that Crat in AgRP neurons has little effect on the intrinsic electrophysiological properties of the cell. Similarly, no genotype-dependent changes in the frequency of spontaneous excitatory or inhibitory post-synaptic potentials (EPSPs or IPSPs, respectively) were detected (Fig 1E-F), indicating no differences in the extrinsic synaptic input in WT compared to KO mice. To show that AgRP neurons require Crat for glucose sensing we recorded AgRP neuronal responses to an increase in extracellular glucose from a basal level of 2mM to 5mM. These glucose concentrations were chosen to represent brain glucose concentrations under fasting and fed conditions, based on glucose concentration estimated in the CSF from fasted and fed rats and mice[33]. Glucose-excited neurons were defined based upon a response characterised by membrane potential depolarization and/or an increase in action potential firing frequency with increased extracellular glucose (Fig1 I). Glucose-inhibited cells were identified by responses to increased glucose characterised by membrane potential hyperpolarisation and/or a reduction in spontaneous action potential firing frequency (Fig1 I). In WT mice, 48% of cells (n=10/21) were excited, 33% of cells (n=7/21) were inhibited and 19% (n=4/21) were insensitive to changes in extracellular glucose (Fig 1G). In KO mice, the number of glucose-excited cells was reduced compared to WT with only 28% classified as glucose excited (n=7/25). Similarly, the incidence of glucose-inhibited cells was reduced to 16% (n=4/25) of the population compared to WT mice with the majority of cells not responding to 5mM glucose 56% (n=14/25) and classified as glucose insensitive (Fig 1H). In total 17/21 AgRP neurons responded to an increase in extracellular glucose in WT mice, whereas as only 11/25 AgRP neurons responded to glucose in KO mice, representing a decrease in glucose-responsive neurons (WT 81% vs KO 44%). These results show Crat deletion impairs intrinsic glucose-sensing capability of AgRP neurons.

Metabolic sensing in AgRP neurons translates low energy state to increase sucrose consumption

Previous studies show that activation of AgRP neurons increases lick bouts for progressively higher concentrations of sucrose and increases the tolerance for bitter tastant in sucrose solution[34]. These studies suggest an inherent physiological ability for AgRP neurons to

detect current energy state and promote the appropriate behavioural response to restore it to equilibrium (or whatever word is appropriate when it comes to energy state). To test this, we used AgRP Crat KO mice, which have impaired glucose sensing and reduced refeeding after fasting[25] and investigated whether Crat deletion affects the rewarding properties of sucrose, using 2-bottle choice experiments. Initial experiments show that WT and KO mice prefer a non-caloric sweetened drink (0.1% saccharin) over water suggesting that Crat deletion does not affect taste perception or causes anhedonia (Fig 2A). We next compared sucrose vs saccharin consumption in fed WT and KO mice and although mice preferred sucrose, there were no genotype differences in either the amount consumed or the preference (Fig 2B, Supp Fig 1A). However, in fasted mice, there was a significantly reduced preference for sucrose in KO compared to WT mice (Fig 2C, see also Supp Fig 1B, E, F; 71.2% vs 93.9% respectively, $p \leq 0.05$).

Bitter tastes such as quinine or denatonium are often used as adulterants to create taste aversions and suppress intake. However, both fasting and AgRP neuronal stimulation drive greater consumption of sucrose in the presence of bitter tastes[34], implying that AgRP neurons are important to detect changes in energy state associated with fasting and prioritise calories over taste. In order to test this, we repeated the sucrose saccharin preference tests but with bitter tasting quinine added to the sucrose solution. Pairing the caloric solution with an unpalatable taste shifts the preference to saccharin in KO, with WT mice showing no preference (Fig 2D, Supp Fig 1C). Strikingly, an overnight fast increases the preference for the quinine-laced sucrose solution in WT, but not in KO mice (Fig 2E, Supp Fig1D), resulting in a significant increase in preference from fed to fasted in WT mice (Fig 2F) but no change in preference in KO mice (Fig 2G). There was no genotype difference in total consumption across the different comparison (Fig 2H), indicating this did not affect preference, and KO mice showed significantly reduced sucrose consumption in a quinine dose response curve (Fig 2I). Collectively, these data show that Crat mediates the ability of AgRP neurons to respond to fasting and increase calorie intake through greater sucrose consumption, even in the presence of quinine to devalue the consumption of sucrose.

Metabolic sensing via Crat in AgRP neurons affects mesolimbic dopamine pathways

Previous studies show that activation of AgRP neurons modulates dopamine release in the NAc[13] and neural encoding of non-caloric and caloric solutions are differentially processed in the NAc and dorsal striatum respectively[35]. Based on the observed differences in sucrose consumption and sucrose/quinine consumption under fasted conditions presented above (Fig 2), we hypothesized that KO mice would show reduced dopamine release in the dorsal striatum. To investigate this, we first employed a positron electron tomography (PET)

method using radiolabelled 18F-fDOPA (Supp Fig 1G). First, we measured dynamic basal dopamine uptake in ventral and dorsal striatum in fasted mice without reward presentation and observed no differences in fDOPA uptake (Supp Fig 1J, K) suggesting Crat deletion in AgRP neurons does not affect baseline uptake parameters. However, in response to peanut butter chip consumption, we detected an increase in fDOPA accumulation 30 minutes after starting in the dorsal striatum of WT but not in KO mice (Supp Fig 1H) and no differences in the ventral striatum (Supp Fig 1I), suggesting that Crat deletion in AgRP neurons restricts a post-ingestive dopamine response to peanut butter chip consumption in the dorsal striatum.

Although this approach provided important information on the uptake of dopamine in the dorsal striatum, it lacks the temporal and spatial resolution to examine acute dopamine release in the NAc or dorsal striatum to food reward approach and consumption. This is an important issue since a study using human subjects showed that there are two temporally and spatially distinct dopamine responses to ingesting a milkshake[36], one immediate orosensory response (to taste) and a second delayed post-ingestive response (to calories). To overcome the resolution issue of our PET/CT scans we switched to *in vivo* fiber photometry measuring dopamine release using the recently developed $GRAB_{DA}$ sensor[28]. This allowed us to measure dopamine signalling in freely behaving mice consuming a peanut butter chip. Acute dopamine release in the NAc was measured using $GRAB_{DA}$ in response to a non-food object (wood dowel), chow food and a peanut butter chip with each presentation separated by 2 mins (presented in that order) (Fig 3A, B) and observed a significant increase in dopamine release in response to chow and peanut butter chip when compared to wood dowel in both fed and fasted WT mice (Fig 3C-J). Strikingly, KO mice did not show a similar significant increase in NAc dopamine release, as assessed by AUC, following chow and a peanut butter chip presentation in the fed state and this was significantly lower compared to WT fed mice (Fig 3E, F). In the fasted state, KO mice showed accumbal dopamine release in response to PB but significantly lower than that seen in WT fasted mice (Fig 3I, J). Time to food contact and time spent eating were not significantly different in WT and KO mice in fed or fasted state (Fig 3P, Q), showing that these factors could not account for differences in dopamine release in the NAc. Furthermore, aligning the dopamine signal to the beginning of peanut butter chip consumption shows that KO mice have diminished dopamine release during peanut butter chip consumption (Fig 3K-O). Taken together, these results highlight that Crat deletion in AgRP neurons reduced acute dopamine release in the NAc in both fed and fasted states in response to chow and a peanut butter chip.

We used the same protocol to measure acute dopamine release in the dorsal striatum in response to a wood dowel, chow food and a peanut butter chip with each presentation separated by 2 mins (Supp Figure 2A, B). Although we observed a main effect for peanut

butter chip to acutely increase dopamine release in the dorsal striatum, there were no significant genotype differences in either the fed or fasted state and no differences in time to contact with a peanut butter chip or time spent eating a peanut butter chip, as assessed by video analysis (Supp Fig 2).

Glucose-sensing via Crat in AgRP neurons affects motivation and dopamine release during operant responding for a sucrose reward

The majority of operant conditioning protocols are conducted in stand-alone operant chambers and typically include a mild calorie restriction to facilitate learning of the instrumental task. This exploits the fact that food restriction enhances appetitive drive, which is a result of elevated AgRP neuronal activity[7,12]. To avoid this potential confound we used the open source FED3[31] operant devices that are placed in the home cage and can be left for long periods of time, which facilities learning in a low stress environment. As such, instrumental learning can be acquired quickly and easily in *ad libitum* fed mice using FED3 devices without the need for caloric restriction – an important consideration for our experiments (Fig 4A). There were no differences in operant responding during FR sessions (Supp Fig 3C), indicating no differences in learning the operant task. In order to test motivation, progressive ratio sessions were performed overnight with (fed) and without access (fasted) to chow. During fed conditions, WT and KO mice displayed similar breakpoint ratios (Fig 4B), however under fasting conditions KO mice showed a reduced breakpoint compared to WT mice. Active (Fig 4C) but not inactive nosepokes (Supp Fig 3B) during the fasted progressive ratio session were significantly lower in KO mice compared to WT, as well as pellets received during the progressive ratio session (Supp Fig 3A). These results demonstrated that Crat deletion in AgRP neurons reduces motivation for sucrose rewards when mice are fasted but not fed, suggesting that the appropriate detection of low energy state by AgRP neurons affects motivation for a palatable food reward.

In order to establish that deficits in motivation were associated with impaired dopamine release in the NAc or dorsal striatum, we used FED3 as it allows for programmable TTL output to synchronize nose poking and pellet retrieval with measurements of dopamine release by $GRAB_{DA}$ photometry (Fig 4D, E). Dopamine release was measured during a progressive ratio allowing us to align dopamine responses to rewarded or non-rewarded nose pokes (see Supp Fig 3D and E for example traces). In fed WT mice, a rewarded nose poke increased NAc dopamine release whereas a non-rewarded nose poke did not (Fig 4F-H). In fed KO mice, we did not observe an increase in accumbal dopamine in response to a rewarded nose poke within the 10 second window (Fig 4G). This was likely due to the significant increase in pellet retrieval time observed in KO fed mice compared to WT fed mice (Supp Fig 3F) without affecting time between nose pokes (Supp Fig 3G, H). In fasted

mice, rewarded nose pokes increased accumbal dopamine release in both WT and KO mice (Fig 4I, J) with a significant main effect for a reduced AUC and max z-score in KO mice in response to a rewarded nose poke (Fig 4K, L). We then aligned photometry data to pellet retrieval to account for any potential differences in pellet retrieval time (Fig 4M-O). AUC and max z-score analysis revealed no significant genotype effects prior to pellet retrieval (Fig 4P, Q), however AUC and max z-score were both significantly reduced in fasted KO mice compared to fasted WT mice after pellet retrieval (Fig 4R, S). These results are consistent with behavioural data showing that reduced accumbal dopamine release in response to pellet retrieval underpins reduced motivation for a palatable food reward in fasted KO mice.

We also examined dopamine release in the dorsal striatum during a progressive ratio schedule (Fig 5A, B). Aligning dorsal striatal dopamine release to rewarded and non-rewarded nose pokes showed an immediate increase in rewarded pokes with no response in non-rewarded pokes (Fig 5C-G). There were no acute differences in dorsal striatal dopamine release between WT and KO mice and there were no differences in release in fed vs fasted mice (Fig 5H, I). When aligned to pellet retrieval, dorsal striatal dopamine peaked immediately prior to retrieval (Fig 5J-L) with no significant differences in AUC or max z-score prior to pellet retrieval between genotypes in fed or fasted states (Fig 5M, N). There was a significant reduction in AUC after pellet retrieval in fasted KO mice compared to fasted WT mice, with no difference for max z-score (Fig 5O, P).

Discussion

While AgRP neurons replicate the actions of hunger on motivated behaviour and midbrain dopamine neurons[7,12-14], the exact mechanism by which these neurons sense hunger to influence dopamine release and motivated behaviour is unknown. In this study, we demonstrate that intact glucose-sensing via Crat in AgRP neurons during fasting is required to increase dopamine release in NAc and dorsal striatum and increased motivated responding for food rewards. The study highlights that hunger-sensing in AgRP neurons potentiates dopamine release in response to food rewards and specifically identifies Crat in AgRP neurons as a potential molecular target to reduce motivation to consume palatable foods.

Deletion of Crat directly impairs glucose-sensing in AgRP neurons. These results are supported by studies deleting Crat from myocytes, as this diminishes the switch from fatty acid metabolism to glucose catabolism after pyruvate administration[37]. The lack of genotype differences in excitatory or inhibitory postsynaptic potentials show that changes in glucose-sensing are not caused by altered synaptic input, but rather reflects changes in the intrinsic glucose-sensing capability of AgRP neurons following Crat deletion. Indeed, an unbiased proteomic survey of AgRP neurons with or without Crat identified numerous differences in proteins regulating synaptic plasticity, particularly in the fasted state[25]. Taken together, our electrophysiological results demonstrated that Crat deletion impairs glucose sensing in AgRP neurons, particularly during low energy states.

AgRP neurons also regulate taste modification in fasted states by potentiating sweet taste sensing at lower sucrose concentrations or by increasing the tolerance of a bitter tastant in sucrose[34]. During fasting, KO mice showed a significantly lower preference for sucrose consumption and a significantly stronger aversion to sucrose laced with quinine compared to WT mice, which did not change during fasting. WT mice, however, increased their preference for sucrose laced with quinine during fasting. These studies indicate that during fasting WT, but not KO mice, seek calories in solutions with low taste appeal, suggesting that KO mice cannot sense the caloric value of sucrose during fasting. This is in line with studies demonstrating that calories are inherently rewarding irrespective of taste[38], implying the inability of KO mice to sense calorie content does not reinforce consumption. Sucrose ingestion is reinforced by dopamine release in the dorsal striatum and NAc and studies demonstrate that dopamine release in the dorsal striatum reinforces the caloric value, whereas dopamine release in the NAc reinforces the hedonic value (taste) of sucrose[35]. Importantly, this study demonstrates that dopamine release in the dorsal striatum (simulating caloric value) can override taste aversion. Similar to this, our PET/CT studies for fDOPA revealed reduced dopamine uptake 30 mins after food reward in KO mice, with no difference in the ventral striatum. We suggest the impaired glucose-sensing capacity of AgRP neurons

485 underlies the reduced dopamine uptake in the dorsal striatum of KO mice, since disrupting
486 glucose oxidation suppressed dorsal striatum dopamine efflux during sugar intake[39]. Thus,
487 we predict that Crat in AgRP neurons is important to detect post-ingestive signals of calorie
488 content and relay this information into relevant dopamine circuits, such as the dorsal
489 striatum. Indeed, AgRP neurons respond within minutes to post-ingestive signals from the
490 gut, such as nutrients and hormones released into the blood or via neural pathways[22-24,40].
491 Studies in humans show palatable food elicits an immediate orosensory dopamine response
492 and a delayed dorsal striatum dopamine response[36]. While the PET/CT scanning approach
493 detected a difference in the dorsal striatum of KO mice after 30 minutes, a major limitation
494 with the PET/CT approach is the lack of temporal resolution around the food approach and
495 consumption, as well as spatial resolution to the NAc. To overcome this, we employed a
496 photometry approach using GRAB^{DA} to measure dopamine release dynamics[28] in the NAc
497 and dorsal striatum before and immediately after food consumption. Although both WT and
498 KO mice spent equal time consuming the peanut butter chip, KO had significantly attenuated
499 dopamine release in the NAc, in fasted state. In the dorsal striatum, we observed
500 coordinated ramping prior to pellet retrieval similar to previous reports[41], but there were no
501 acute differences in the dorsal striatum dopamine release. Thus, our studies demonstrate
502 that acute fasting-induced release of dopamine in the NAc to a palatable food reward
503 requires metabolic input from AgRP neurons.
504 Importantly, Crat deletion in AgRP neurons also attenuated progressive ratio operant
505 responding for sucrose rewards during fasting with KO mice showing reduced breakpoint
506 ratio, active nose pokes and pellets consumed. Although the motivation to obtain food is
507 associated with activation of AgRP neurons[7,12], our studies provide a molecular mechanism
508 responsible for translating low energy availability into a dopamine-driven motivational action
509 to consume sucrose. We used a home-cage operant self-administration approach by placing
510 FED3 in the home cages of mice. This provides advantages such as reducing handling
511 stress, but most importantly, mice did not require food restriction to learn the action-outcome
512 (nose poke-sucrose pellet) contingency and there were no differences in acquisition rates
513 between WT and KO mice. This was important because differential responses to food
514 restriction, as shown previously[25,42], may have impaired subsequent responding during the
515 progressive ratio tests.
516 Using FED3 coupled with GRAB$_{DA}$ we measured dopamine release in the NAc or dorsal
517 striatum during a progressive ratio session in response to rewarded and non-rewarded nose
518 pokes. In the NAc, dopamine release increased prior to pellet retrieval and while there were
519 no differences in AUC or max z-score prior to pellet retrieval, both these parameters were
520 significantly reduced in KO mice under fasted conditions. The combination of reduced
521 breakpoint responding and lower dopamine release in the NAc to pellet retrieval is

consistent with the known role of NAc dopamine release to drive food seeking[43] and to assign an appropriate investment of effort to the available reward[44-46]. In the dorsal striatum, dopamine ramping was observed prior to pellet retrieval without any genotype differences, which dropped to baseline soon after pellet retrieval consistent with previous reports[41]. Interestingly, AUC analysis after pellet retrieval suggest KO mice have a faster return to baseline, although how this might reflect reduced motivational drive is unknown. When considered together, both $GRAB_{DA}$ photometry and PET/CT studies with fDOPA reveal KO mice have deficits in acute orosensory NAc dopamine release and long-term post-ingestive dorsal striatum dopamine release, similar to studies conducted in humans[36]. Thus, we predict both reduced acute dopamine release in the NAc in response to pellet retrieval and longer-term deficits in dopamine uptake in the dorsal striatum (30 mins) underlie reduced motivational drive to consume sucrose rewards in KO, compared to WT mice.

Most of the observed deficits in KO mice in the present study manifested in the fasted state, including changes in glucose-sensing, sucrose preference, NAc dopamine release and during progressive ratio operant responding. Our previous studies showed that deletion of Crat from AgRP neurons reduced food intake after fasting, impaired the AgRP proteomic response to fasting and impaired homeostatic changes to calorie restriction and time-restricted feeding[25,42,47]. Taken together, these studies highlight the major role of Crat in AgRP neurons is to facilitate the metabolic adaptation to low energy availability. This is unsurprising given AgRP neurons respond to low energy availability by increasing firing frequency and gene transcription[16-20] in order to maintain hunger signaling and appetitive motivation. The importance of AgRP neurons to respond to hunger is underscored by the starvation caused following genetic ablation of AgRP neurons[6,8].

An unanswered question remains, as to how AgRP neurons influence mesolimbic dopamine signaling. Given that very few, if any, AgRP terminals are found in the VTA[14], it seems unlikely that AgRP neurons directly affect dopaminergic neurons in the VTA. In addition, dissociable dopamine dynamics differentially regulate learning and motivational properties, with dopamine release in NAc underlying motivational properties and VTA firing properties underlying learning properties[46]. Based on these observations, AgRP neurons presumably influence mechanisms in the NAc that promote dopamine release. Although the MC4R is found in the NAc[48], there is little evidence to suggest activation of AgRP directly targets neurons in the NAc. Activation of AgRP nerve terminals in the lateral hypothalamus (LH), but not the paraventricular hypothalamic nucleus, increased taste reactivity to sucrose[34], suggesting the LH may be an indirect route, through which AgRP neurons influence mesolimbic dopamine release. This is consistent with the known role of the LH in mediating appetitive motivation and food consumption[49]. Finally, the suppression of AgRP neuronal activity with food presentation occurs prior to consumption[11,18,21] and this coincides with

559 increased NAc and dorsal striatum dopamine release prior to pellet consumption. Whether
560 or not these changes are functionally related remains to be determined but activation of
561 AgRP neurons also drives dopamine release in the NAc[13] so a number of questions remain
562 to be answered, as to how AgRP neurons facilitate dopamine release.
563 In summary, we show that Crat in AgRP neurons is required 1) for appropriate glucose-
564 sensing, 2) to transmit fasting-induced metabolic information to dopamine release in the NAc
565 and dorsal striatum, albeit over different time frames and 3) to increased motivated
566 behaviour for sucrose rewards. Since the motivation to eat depends not only on the
567 palatability of food, but also metabolic state[50,51], these studies identify a novel molecular
568 target in hunger-sensing AgRP neurons to control the overconsumption of palatable foods.
569 Whether or not this plays an important role in obesity remains to be determined since
570 obesity desensitizes AgRP neurons to food cues and metabolic feedback[52]. However, the
571 observation that fasting increases NAc dopamine release in response to high fat diet, when
572 compared to chow diet[15], suggests that homeostatic circuits might play an important role in
573 the pathogenesis of obesity. Future research is required to disentangle how homeostatic
574 signals influence food reward processing and how this contributes to obesity.
575
576
577
578
579
580
581
582
583
584
585
586

REFERENCES

1 Sih, A. Optimal behavior: can foragers balance two conflicting demands? *Science* **210**, 1041-1043, (1980).

2 Whitham, J. & Mathis, A. Effects of hunger and predation risk on foraging behavior of graybelly salamanders, Eurycea multiplicata. *J Chem Ecol* **26**, 1659-1665, (2000).

3 Goldstone, A. P. *et al.* Fasting biases brain reward systems towards high-calorie foods. *Eur J Neurosci* **30**, 1625-1635, (2009).

4 Cameron, J. D., Goldfield, G. S., Finlayson, G., Blundell, J. E. & Doucet, E. Fasting for 24 hours heightens reward from food and food-related cues. *PLoS One* **9**, e85970, (2014).

5 Aponte, Y., Atasoy, D. & Sternson, S. M. AGRP neurons are sufficient to orchestrate feeding behavior rapidly and without training. *Nature neuroscience* **14**, 351-355, (2011).

6 Gropp, E. *et al.* Agouti-related peptide-expressing neurons are mandatory for feeding. *Nature Neuroscience* **8**, 1289-1291, (2005).

7 Krashes, M. J. *et al.* Rapid, reversible activation of AgRP neurons drives feeding behavior in mice. *J Clin Invest* **121**, 1424-1428, (2011).

8 Luquet, S., Perez, F. A., Hnasko, T. S. & Palmiter, R. D. NPY/AgRP neurons are essential for feeding in adult mice but can be ablated in neonates. *Science* **310**, 683-685, (2005).

9 Ruan, H. B. *et al.* O-GlcNAc transferase enables AgRP neurons to suppress browning of white fat. *Cell* **159**, 306-317, (2014).

10 Atasoy, D., Betley, J. N., Su, H. H. & Sternson, S. M. Deconstruction of a neural circuit for hunger. *Nature* **488**, 172-177, (2012).

11 Betley, J. N. *et al.* Neurons for hunger and thirst transmit a negative-valence teaching signal. *Nature* **521**, 180-185, (2015).

12 Chen, Y. M., Lin, Y. C., Zimmerman, C. A., Essner, R. A. & Knight, Z. A. Hunger neurons drive feeding through a sustained, positive reinforcement signal. *eLife* **5**, (2016).

13 Alhadeff, A. L. *et al.* Natural and Drug Rewards Engage Distinct Pathways that Converge on Coordinated Hypothalamic and Reward Circuits. *Neuron* **103**, 891-+, (2019).

14 Dietrich, M. O. *et al.* AgRP neurons regulate development of dopamine neuronal plasticity and nonfood-associated behaviors. *Nat Neurosci* **15**, 1108-1110, (2012).

15 Mazzone, C. M. *et al.* High-fat food biases hypothalamic and mesolimbic expression of consummatory drives. *Nature Neuroscience* **23**, 1253-+, (2020).

16 Baskin, D. G., Breininger, J. F. & Schwartz, M. W. Leptin receptor mRNA identifies a subpopulation of neuropeptide Y neurons activated by fasting in rat hypothalamus. *Diabetes* **48**, 828-833, (1999).

17 Briggs, D. I., Lemus, M. B., Kua, E. & Andrews, Z. B. Diet-induced obesity attenuates fasting-induced hyperphagia. *J Neuroendocrinol* **23**, 620-626, (2011).

18 Mandelblat-Cerf, Y. *et al.* Arcuate hypothalamic AgRP and putative POMC neurons show opposite changes in spiking across multiple timescales. *eLife* **4**, (2015).

19 Schwartz, M. W., Erickson, J. C., Baskin, D. G. & Palmiter, R. D. Effect of fasting and leptin deficiency on hypothalamic neuropeptide Y gene transcription in vivo revealed by expression of a lacZ reporter gene. *Endocrinology* **139**, 2629-2635, (1998).

20 Yang, Y., Atasoy, D., Su, H. H. & Sternson, S. M. Hunger states switch a flip-flop memory circuit via a synaptic AMPK-dependent positive feedback loop. *Cell* **146**, 992-1003, (2011).

21 Chen, Y., Lin, Y. C., Kuo, T. W. & Knight, Z. A. Sensory detection of food rapidly modulates arcuate feeding circuits. *Cell* **160**, 829-841, (2015).

22 Su, Z. W., Alhadeff, A. L. & Betley, J. N. Nutritive, Post-ingestive Signals Are the Primary Regulators of AgRP Neuron Activity. *Cell reports* **21**, 2724-2736, (2017).

23 Beutler, L. R. *et al.* Dynamics of Gut-Brain Communication Underlying Hunger. *Neuron* **96**, 461-+, (2017).

24 Goldstein, N. *et al.* Hypothalamic detection of macronutrients via multiple gut-brain pathways. *Cell Metabolism* **33**, 1-12, (2021).

25 Reichenbach, A. *et al.* AgRP Neurons Require Carnitine Acetyltransferase to Regulate Metabolic Flexibility and Peripheral Nutrient Partitioning. *Cell reports* **22**, 1745-1759, (2018).

26 Kinahan, P. E. & Fletcher, J. W. Positron Emission Tomography-Computed Tomography Standardized Uptake Values in Clinical Practice and Assessing Response to Therapy. *Semin Ultrasound Ct* **31**, 496-505, (2010).

27 Mani, B. K. *et al.* The role of ghrelin-responsive mediobasal hypothalamic neurons in mediating feeding responses to fasting. *Mol Metab* **6**, 882-896, (2017).

28 Sun, F. M. *et al.* A Genetically Encoded Fluorescent Sensor Enables Rapid and Specific Detection of Dopamine in Flies, Fish, and Mice. *Cell* **174**, 481-+, (2018).

29 Lerner, T. N. *et al.* Intact-Brain Analyses Reveal Distinct Information Carried by SNc Dopamine Subcircuits. *Cell* **162**, 635-647, (2015).

30 Barker, D. J. *et al.* Lateral Preoptic Control of the Lateral Habenula through Convergent Glutamate and GABA Transmission. *Cell reports* **21**, 1757-1769, (2017).

31 Matikainen-Ankney, B. A. *et al.* Feeding Experimentation Device version 3 (FED3): An open-source home-cage compatible device for measuring food intake and operant behavior. *bioRxiv*, (2020).

32 Richardson, N. R. & Roberts, D. C. S. Progressive ratio schedules in drug self-administration studies in rats: A method to evaluate reinforcing efficacy. *J Neurosci Methods* **66**, 1-11, (1996).

33 van den Top, M. *et al.* The impact of ageing, fasting and high-fat diet on central and peripheral glucose tolerance and glucose-sensing neural networks in the arcuate nucleus. *J Neuroendocrinol* **29**, (2017).

34 Fu, O. *et al.* Hypothalamic neuronal circuits regulating hunger-induced taste modification. *Nature communications* **10**, (2019).

35 Tellez, L. A. *et al.* Separate circuitries encode the hedonic and nutritional values of sugar. *Nature Neuroscience* **19**, 465-+, (2016).

36 Thanarajah, S. E. *et al.* Food Intake Recruits Orosensory and Post-ingestive Dopaminergic Circuits to Affect Eating Desire in Humans. *Cell Metabolism* **29**, 695-+, (2019).

37 Muoio, D. M. *et al.* Muscle-specific deletion of carnitine acetyltransferase compromises glucose tolerance and metabolic flexibility. *Cell Metab* **15**, 764-777, (2012).

38 de Araujo, I. E. *et al.* Food reward in the absence of taste receptor signaling. *Neuron* **57**, 930-941, (2008).

39 Tellez, L. A. *et al.* Glucose utilization rates regulate intake levels of artificial sweeteners. *J Physiol-London* **591**, 5727-5744, (2013).

40 Bai, L. *et al.* Genetic Identification of Vagal Sensory Neurons That Control Feeding. *Cell* **179**, 1129-+, (2019).

41 London, T. D. *et al.* Coordinated Ramping of Dorsal Striatal Pathways preceding Food Approach and Consumption. *Journal of Neuroscience* **38**, 3547-3558, (2018).

42 Reichenbach, A. *et al.* Carnitine Acetyltransferase in AgRP Neurons Is Required for the Homeostatic Adaptation to Restricted Feeding in Male Mice. *Endocrinology* **159**, 2473-2483, (2018).

43 Roitman, M. F., Stuber, G. D., Phillips, P. E. M., Wightman, R. M. & Carelli, R. M. Dopamine operates as a subsecond modulator of food seeking. *Journal of Neuroscience* **24**, 1265-1271, (2004).

44 Hamid, A. A. *et al.* Mesolimbic dopamine signals the value of work. *Nature Neuroscience* **19**, 117-+, (2016).

45 Howe, M. W., Tierney, P. L., Sandberg, S. G., Phillips, P. E. M. & Graybiel, A. M. Prolonged dopamine signalling in striatum signals proximity and value of distant rewards. *Nature* **500**, 575-+, (2013).
46 Mohebi, A. *et al.* Dissociable dopamine dynamics for learning and motivation. *Nature* **570**, 65-+, (2019).
47 Reichenbach, A. *et al.* Carnitine acetyltransferase (Crat) in hunger-sensing AgRP neurons permits adaptation to calorie restriction. *FASEB J*, fj201800634R, (2018).
48 Lim, B. K., Huang, K. W., Grueter, B. A., Rothwell, P. E. & Malenka, R. C. Anhedonia requires MC4R-mediated synaptic adaptations in nucleus accumbens. *Nature* **487**, 183-U164, (2012).
49 Stuber, G. D. & Wise, R. A. Lateral hypothalamic circuits for feeding and reward. *Nature Neuroscience* **19**, 198-205, (2016).
50 Sun, X. *et al.* The neural signature of satiation is associated with ghrelin response and triglyceride metabolism. *Physiology & Behavior* **136**, 63-73, (2014).
51 Simon, J. J. *et al.* Integration of homeostatic signaling and food reward processing in the human brain. *Jci Insight* **2**, (2017).
52 Beutler, L. R. *et al.* Obesity causes selective and long-lasting desensitization of AgRP neurons to dietary fat. *eLife* **9**, (2020).

FIGURE LEGENDS

Figure 1: Crat deletion impairs glucose responsiveness of AgRP neurons. Intrinsic electrophysiological properties were little affected in KO versus WT mice including: resting membrane potential (A), input resistance (B), spontaneous action potential firing frequency (C), action potential amplitude (D). Spontaneous excitatory (E) and inhibitory (F) post-synaptic potentials compared in WT and KO mice in response to an increase in glucose from 2mM to 5mM. Glucose responsive profiles of AgRP neurons from WT and KO mice characterised by their response to increased extracellular glucose concentration from 2mM to 5mM (G-H). Sample traces showing examples of glucose excited (top) and glucose inhibited (bottom) neurons in response to an increase in glucose from 2 to 5mM glucose. Data +/- SEM, two-way ANOVA with Tukey's post hoc analysis and unpaired students t-test; a, significant at $p<0.05$.

Figure 2: Mice lacking Crat in AgRP neurons choose taste over calories during fasting. In a 2-bottle choice paradigm, mice had *ad libitum* access to chow for 4 days followed by an overnight fast. Position of bottles were swapped daily and volume consumed overnight recorded. Bottles were washed after each choice pair and mice had 2 days of water in both bottles. Dark coloured dots represent female mice (6 WT, 6 KO), shaded dots male mice (5 WT, 7 KO). Pie charts show preference for saccharin (light blue) and comparator solution (dark blue). After acclimation to the BioDaq cages, mice received choice of water and 0.1% saccharin (A), 4% sucrose and 0.1% saccharin (B+C) or 4% sucrose laced with 0.1mM Quinine and 0.1% saccharin (D+E). Change in preference towards caloric quinine /sucrose solution during fasting in WT (F) and KO (G). Combined fluid consumption for each part of the experiment (H) and dose response curve for higher quinine concentrations in 4% sucrose solution from different cohorts of mice (n=5-14). (I). Data +/- SEM, two-way ANOVA with Tukey's post hoc analysis and unpaired students t-test; a, significant at $p<0.05$.

Figure 3: deficits in glucose sensing in AgRP neurons affects dopamine signalling. Experimental design to examine dopamine signalling in Nucleus accumbens. (A): Female (3 WT, 4 KO) and male (4 WT, 4 KO) mice trained to receive peanut butter chips were tethered to a fiber optic cable in their home cage and allowed time to acclimatize to it. Then the dopamine response to a wood dowel (a, black), standard chow (b, tangerine), and peanut butter chip (c, blue) were measured. Schematic of $GRAB_{DA}$ (AAV-hSyn-DA4.3) injection site in the Nucleus accumbens and fiber placement (B). Average dopamine traces aligned to object dropping into cage of fed (C+D) and fasted (G+H) mice and AUC (E+I) and max z-Score (F+J) of the dopamine signal in response to it. Average dopamine traces aligned to

749 first contact with peanut butter chip from fed (K) and fasted (L) mice, individual traces in
750 heatmap (M), AUC (N) and max z-Score during peanut butter consumption. Time passed
751 between drop and contact with peanut butter (P) and time spent eating (Q). Data +/- SEM,
752 two-way ANOVA with Tukey's post hoc analysis; a, significant at $p<0.05$
753
754 **Figure 4:** deficits in AgRP glucose sensing affects motivation for sucrose rewards during
755 fasting. Mice (8 WT, 9 KO) were trained to nose poke for sucrose rewards using fixed ratio
756 schedule (FR1, FR3, FR5) to reliably nose poke on average 75% correct for 3 consecutive
757 nights before undergoing PR schedules with or without chow accessible (A). Break point
758 from fed and fasted mice (B) and correct nose pokes of fasting PR session (C). Schematic of
759 $GRAB_{DA}$ (AAV-hSyn-DA4.3) injection site in the Nucleus accumbens and fiber placement
760 (D). Experimental design (E): mice with fiber implant (same as in Figure 3) were trained to
761 nose poke as described and tethered to a fiber optic cable in their home cage with FED3 not
762 accessible. After 5 min acclimation mice gained access to FED3 on PR schedule. Combined
763 average dopamine response of rewarded and non-rewarded correct nose pokes of 4 WT (F)
764 and 4 KO (G) in fed state and 7 WT (I) and 6 KO (J) after overnight fast and heat map
765 showing each rewarded nose poke(H). AUC (K) and max z-Score (L) of rewarded nose
766 pokes. Average dopamine response to pellet retrieval in fed state (M) and after overnight
767 fast (N) and heatmap showing individual responses (O). AUC (P+R) and max z-Score (Q+S)
768 of dopamine traces prior to (-5 to 0 sec) and post (0 to 10 sec) pellet retrieval. Data +/- SEM,
769 two-way ANOVA with Tukey's post hoc analysis; a, significant at $p<0.05$
770
771 **Figure 5.** AgRP glucose sensing is not required for dopamine signaling in the dorsal
772 striatum for operant conditioning.
773 Schematic of $GRAB_{DA}$ (AAV-hSyn-DA4.3) injection site in the dorsal striatum and fiber
774 placement (A). Experimental design (B): mice with fiber implant were trained to nose poke
775 as described and tethered to a fiber optic cable in their home cage with FED3 not
776 accessible. After 5 min acclimation mice gained access to FED3 on PR schedule. Combined
777 average dopamine response of rewarded and non-rewarded correct nose pokes of 4 WT (C)
778 and 4 KO (D) in fed state and 4 WT (F) and 4 KO (G) after overnight fast and heat map
779 showing each rewarded nose poke (E). AUC (H) and max z-Score (I) of rewarded nose
780 pokes. Average dopamine response to pellet retrieval in fed state (J) and after overnight fast
781 (K) and heatmap showing individual responses (L). AUC (M+O) and max z-Score (N+P) of
782 dopamine traces before (-5 to 0 sec) and after (0 to 10 sec) pellet retrieval. Data +/- SEM,
783 two-way ANOVA with Tukey's post hoc analysis; a, significant at $p<0.05$
784
785

786

787

788

SUPPLEMENTARY FIGURE LEGENDS

Supplementary Figure 1

Saccharin Preference score for sucrose vs saccharin choice fed (A) and fasted (B), and for quinine/sucrose vs saccharin fed (C) and fasted (D). Change in preference towards sucrose with fasting in WT (E) and KO (F).

Experimental design for fDOPA PET scan (G): Mice were trained to receive Reese® peanut butter chips and then overnight fasted. On the experimental day, mice received ip injection of benserazide and entacapone to prevent peripheral breakdown of fDOPA (iv injection 30 min afterwards). Mice were allowed to recover 5 min and then given 1 peanut butter chip, which they ate within 5 min. Then mice were anaesthetised and prepared for PET/CT scan and dopamine uptake in dorsal (H) and ventral striatum (I) measured. Baseline fDOPA uptake in dorsal striatum (J) and ventral striatum (K). Two-way ANOVA with Tukey's post hoc analysis and unpaired students t-test; a, significant at $p<0.05$

Supplementary Figure 2

Deficits in glucose sensing in AgRP neurons does not affect acute dopamine release in the dorsal striatum. Experimental design to examine dopamine signalling in dorsal striatum (A): Female (2 WT, 3 KO) and male (4 WT, 4 KO) mice trained to receive peanut butter chips were tethered to a fiber optic cable in their home cage and allowed time to acclimatize to it. Then the dopamine response to a wood dowel (a, black), standard chow (b, tangerine), and peanut butter chip (c, blue) were measured. Schematic of $GRAB_{DA}$ (AAV-hSyn-DA4.3) injection site in the dorsal striatum and fiber placement (B). Average dopamine traces aligned to object dropping into cage of fed (C+D) and fasted (G+H) mice and AUC (E+I) and max z-Score (F+J) of the dopamine signal in response to it. Average dopamine traces aligned to first contact with peanut butter chip from fed (K) and fasted (L) mice, individual traces in heatmap (M), AUC (N) and max z-Score during peanut butter consumption. Time passed between drop and contact with peanut butter (P) and time spent eating (Q). Two-way ANOVA with Tukey's post hoc analysis; a, significant at $p<0.05$

Supplementary Figure 3.

Received pellets during PR sessions (A) and incorrect nose pokes during fasting PR session over time (B). FR1, FR 3 and FR 5 training data (C). Example traces of fiber photometry recordings from the nucleus accumbens during PR sessions (blue line indicates correct nose pokes; pink lines represent pellet retrieval) in WT (D) and KO (E) after overnight fast. Time between rewarded poke and pellet retrieval (F), time between all correct nose pokes (G) and time between first 4 nose pokes (H) note the time scales are logarithmic. Two-way ANOVA with Tukey's post hoc analysis; a, significant at $p<0.05$

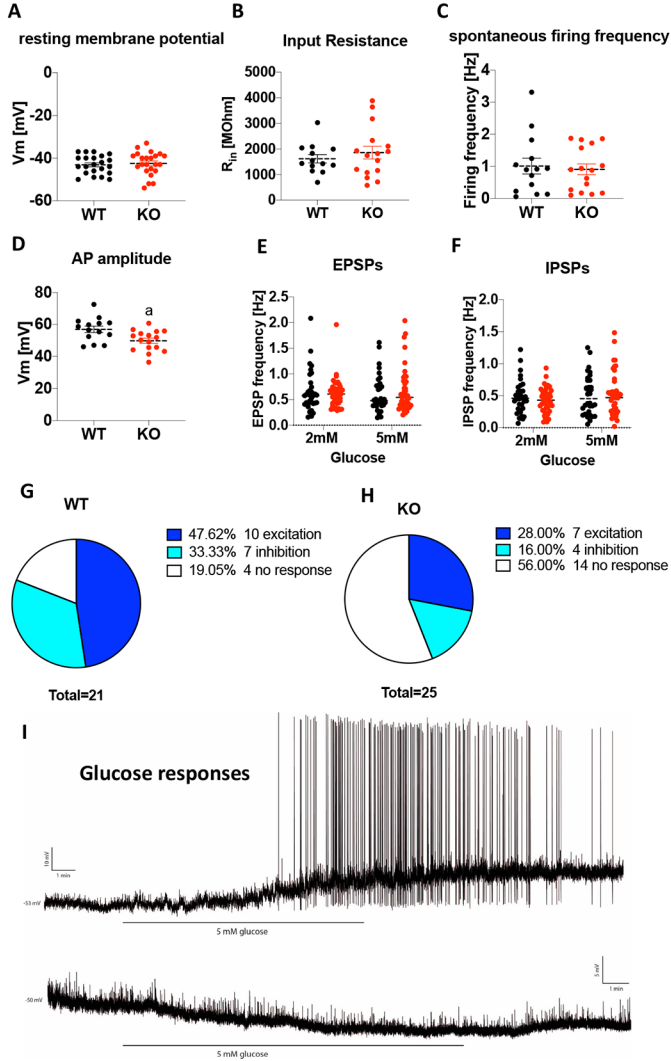
A
resting membrane potential
Vm [mV]
0
-20
-40
-60
WT
KO
B
Input Resistance
R_{in} [MOhm]
5000
4000
3000
2000
1000
0
WT
KO
C
spontaneous firing frequency
Firing frequency [Hz]
4
3
2
1
0
WT
KO
D
AP amplitude
Vm [mV]
80
60
40
20
0
a
WT
KO
E
EPSPs
EPSP frequency [Hz]
2.5
2.0
1.5
1.0
0.5
0.0
2mM
5mM
Glucose
F
IPSPs
IPSP frequency [Hz]
2.0
1.5
1.0
0.5
0.0
2mM
5mM
Glucose
G
WT
47.62% 10 excitation
33.33% 7 inhibition
19.05% 4 no response
Total=21
H
KO
28.00% 7 excitation
16.00% 4 inhibition
56.00% 14 no response
Total=25
I
Glucose responses
10 mV
1 min
-53 mV
5 mM glucose
5 mV
1 min
-50 mV
5 mM glucose

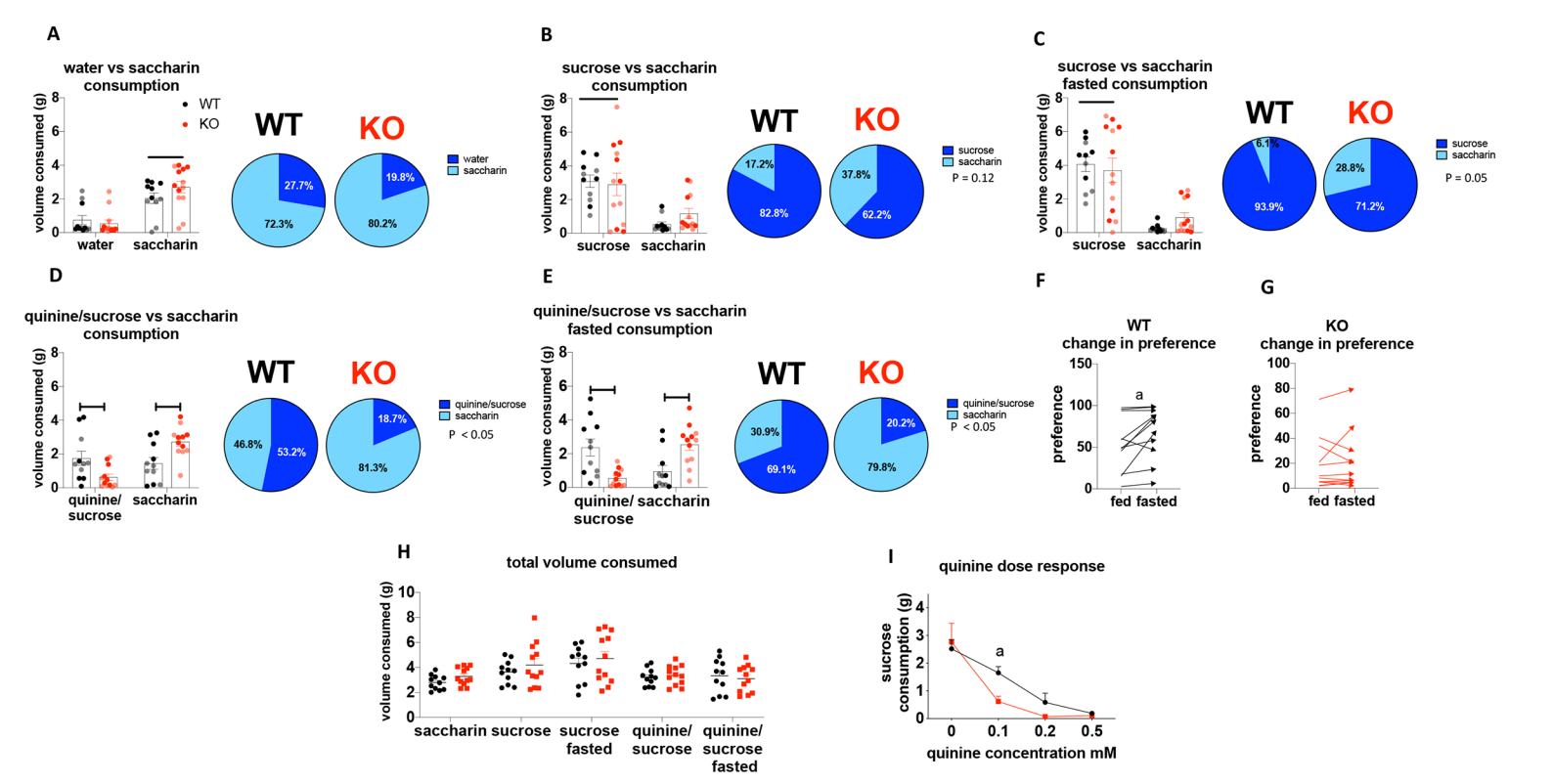
A
water vs saccharin consumption
WT
KO
volume consumed (g)
water
saccharin
WT
KO
27.7%
72.3%
19.8%
80.2%
water
saccharin
B
sucrose vs saccharin consumption
volume consumed (g)
sucrose
saccharin
WT
KO
17.2%
82.8%
37.8%
62.2%
sucrose
saccharin
P = 0.12
C
sucrose vs saccharin fasted consumption
volume consumed (g)
sucrose
saccharin
WT
KO
6.1%
93.9%
28.8%
71.2%
sucrose
saccharin
P = 0.05
D
quinine/sucrose vs saccharin consumption
volume consumed (g)
quinine/ sucrose
saccharin
WT
KO
46.8%
53.2%
18.7%
81.3%
quinine/sucrose
saccharin
P < 0.05
E
quinine/sucrose vs saccharin fasted consumption
volume consumed (g)
quinine/ sucrose
saccharin
WT
KO
30.9%
69.1%
20.2%
79.8%
quinine/sucrose
saccharin
P < 0.05
F
WT
change in preference
preference
a
fed
fasted
G
KO
change in preference
preference
fed
fasted
H
total volume consumed
volume consumed (g)
saccharin
sucrose
sucrose fasted
quinine/ sucrose
quinine/ sucrose fasted
I
quinine dose response
sucrose consumption (g)
a
quinine concentration mM

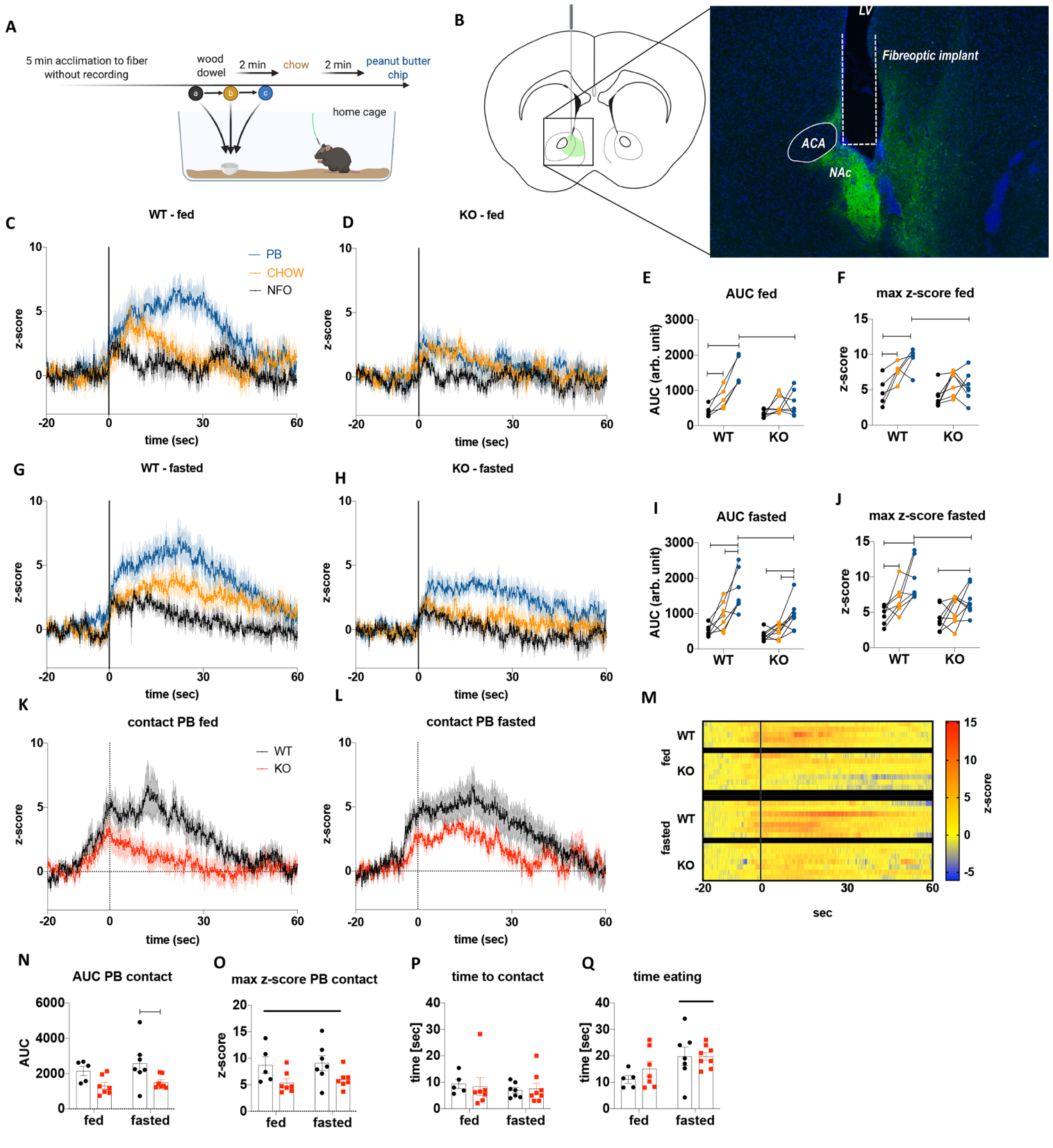
A
5 min acclimation to fiber without recording
wood dowel
2 min
chow
2 min
peanut butter chip
a
b
c
home cage
B
LV
Fibreoptic implant
ACA
NAc
C
WT - fed
PB
CHOW
NFO
z-score
time (sec)
D
KO - fed
E
AUC fed
AUC (arb. unit)
WT
KO
F
max z-score fed
G
WT - fasted
H
KO - fasted
I
AUC fasted
J
max z-score fasted
K
contact PB fed
L
contact PB fasted
M
fed
fasted
sec
N
AUC PB contact
O
max z-score PB contact
P
time to contact
time [sec]
Q
time eating

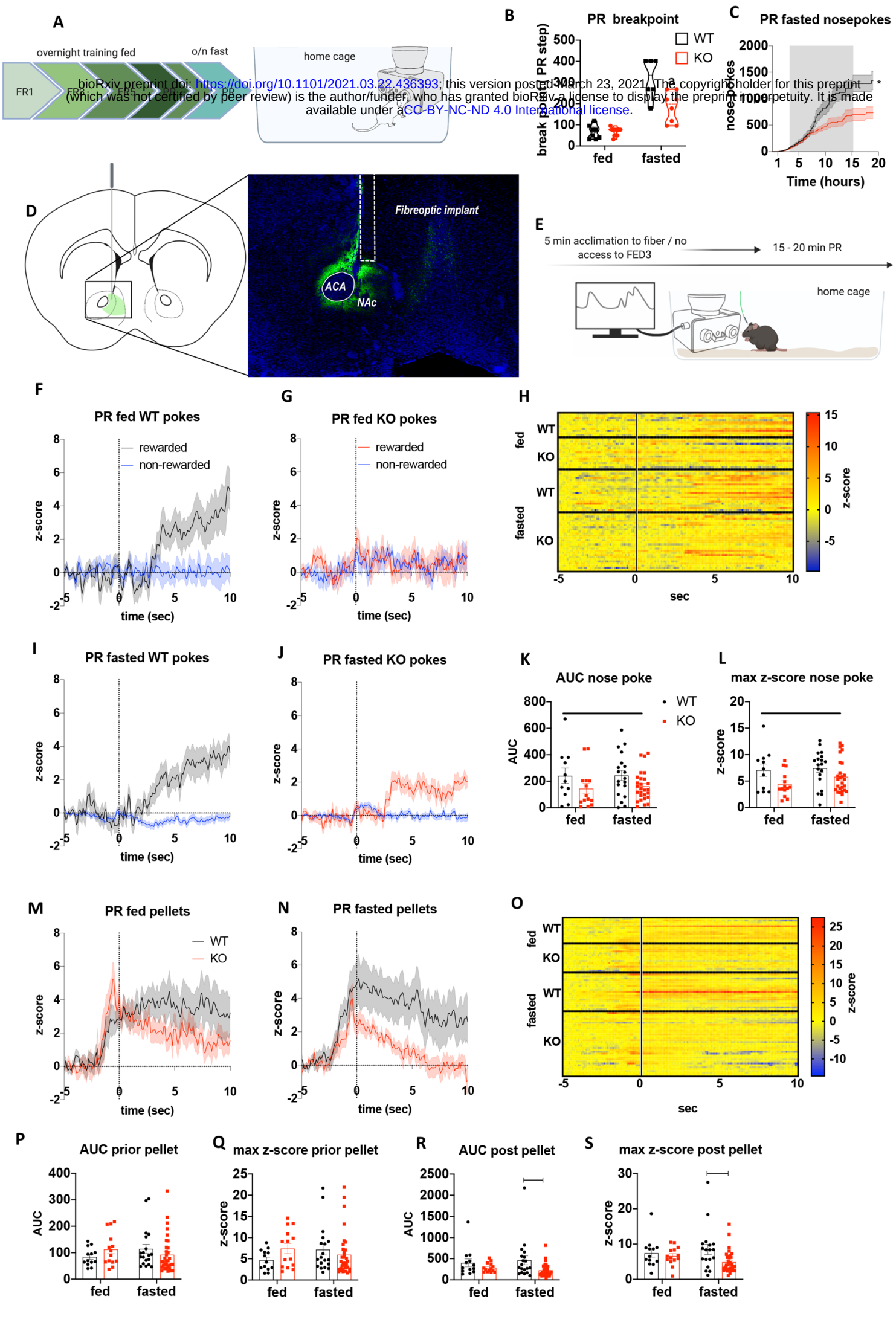

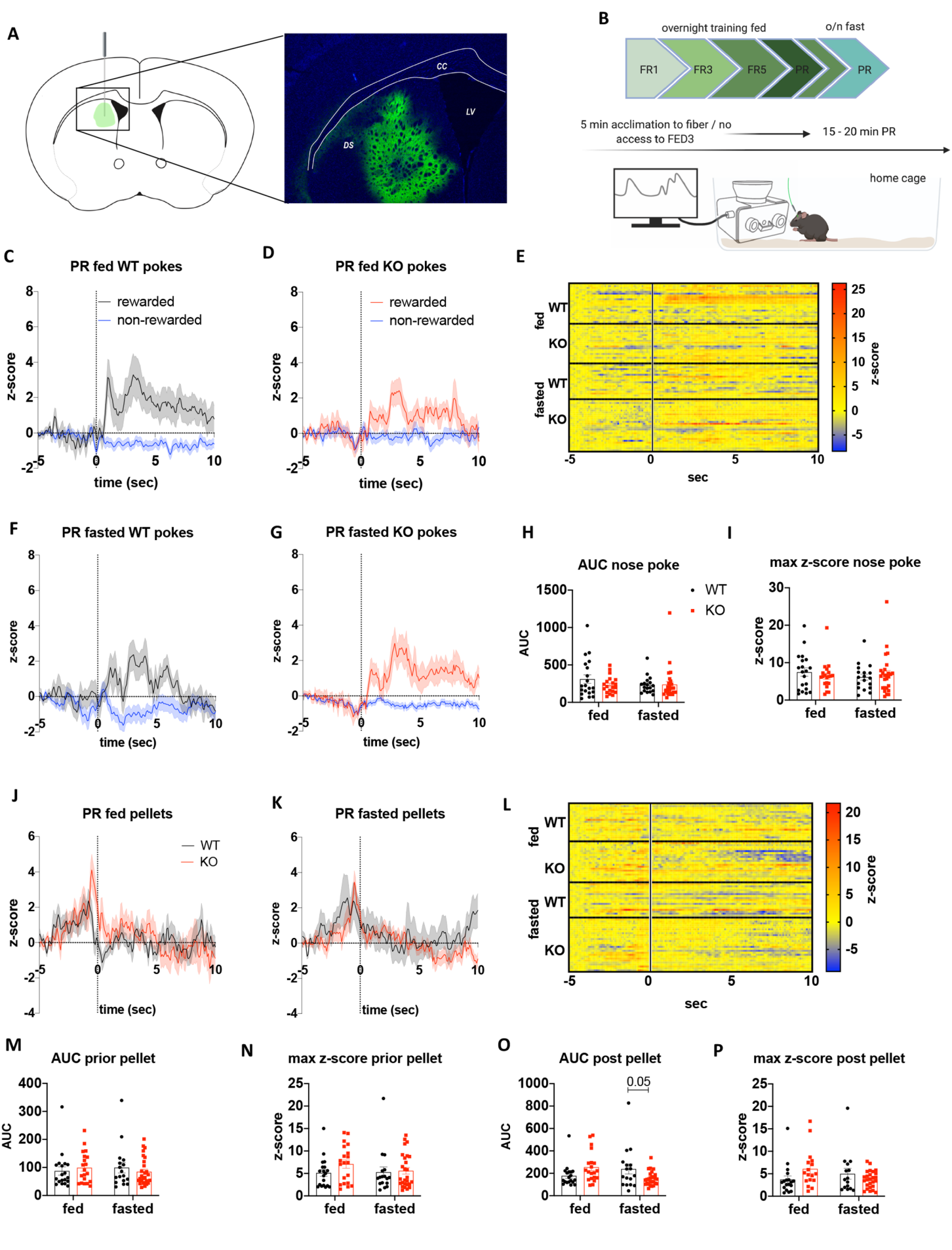
A
CC
LV
DS
B
overnight training fed
o/n fast
FR1
FR3
FR5
PR
PR
5 min acclimation to fiber / no access to FED3
15 - 20 min PR
home cage
C
PR fed WT pokes
rewarded
non-rewarded
z-score
time (sec)
D
PR fed KO pokes
rewarded
non-rewarded
z-score
time (sec)
E
fed
WT
KO
fasted
WT
KO
z-score
sec
F
PR fasted WT pokes
z-score
time (sec)
G
PR fasted KO pokes
z-score
time (sec)
H
AUC nose poke
WT
KO
AUC
fed
fasted
I
max z-score nose poke
z-score
fed
fasted
J
PR fed pellets
WT
KO
z-score
time (sec)
K
PR fasted pellets
z-score
time (sec)
L
fed
WT
KO
fasted
WT
KO
z-score
sec
M
AUC prior pellet
AUC
fed
fasted
N
max z-score prior pellet
z-score
fed
fasted
O
AUC post pellet
0.05
AUC
fed
fasted
P
max z-score post pellet
z-score
fed
fasted